Streamwise Corner Flow with Wall Suction

W. H. Barclay*
University College London, London, England
and
H. A. El-Gamal
University of Alexandria, Alexandria, Egypt

Solutions are presented for the flow along a rectangular streamwise corner when suction is applied at the corner surface. The suction is uniform everywhere except in the vicinity of the apex of the corner, where the no-slip condition requires that the velocity vector vanish. Exact solutions are given respectively for small and large values of a suction parameter σ, as well as an approximate solution for arbitrary σ. For large σ the approximate and exact solutions are in excellent agreement and evidence is presented to support the hypothesis that the approximate solution is practically useful everywhere beyond the range of the exact solution for small σ.

Introduction

A RECTANGULAR streamwise corner is depicted in Fig. 1, wherein the corner is formed by the abutment of two quarter-infinite rigid planes along a streamwise edge. The flow along such a corner is at once interesting and important. Near the abutment the flow is essentially three-dimensional in character as a result of the interaction between the otherwise two-dimensional boundary layers on the plates. Furthermore, the no-slip condition on the plates implies that the gradient of the streamwise component of the velocity vector is zero at the abutment, thereby giving rise to a streamwise velocity profile in the symmetry plane reminiscent of the separation point profile in flat plate flows. Although such a profile does not necessarily imply separation in corner flows, it does suggest a precariously stable corner layer at best, and that this is the case for laminar flows at least has been a feature of experimental work in this field.[1,2]

Laminar flow along the "sharp" rectangular streamwise corner is now quite well understood[3,4] and this understanding has been extended to corners other than rectangular.[5] Work has also been done on corners where the infinite transverse curvature at the joining line of the plates is replaced by a region of finite curvature effecting a smooth transition from one plate to the other.[6] These so-called "radiused" corners are probably a little nearer to the situations encountered in practice and include the "sharp" corners as special cases. The removal of the line of infinite transverse curvature almost certainly improves the stability of the flow for corners whose angles are less than 180 deg. (For angles greater than 180 deg stability does not seem to be a problem.)

Alteration to the corner geometry clearly affords one means for modifying the flow regime and is worthy of consideration. Another approach is to use boundary-layer suction through porous corner surfaces. This technique, although not always easy to institute in practice, has a much greater potential for conferring resistance to separation than does geometrical change. It also has other advantages for the flow in narrow passages such as occur in low aspect ratio compressor blade rows. El-Gamal and Barclay[7] have considered a special case of rectangular corner flow with wall suction. The suction was assumed to be independent of the streamwise coordinate and they dealt with the problem only in its far downstream limit where the two-dimensional boundary layers on the corner plates have reached a constant state.[8] The corner layer also assumes a constant state in this limit and for a particular choice of wall suction transverse distribution within the corner layer they obtained the crossflow velocity components in closed form, leaving a very simple numerical problem for the streamwise velocity component. El-Gamal and Barclay[9] have also determined the "side-edge" boundary conditions for uniform suction throughout the length of the corner.

In the present paper solutions are obtained for flow with suction independent of the streamwise coordinate which are valid more extensively along the corner and somewhat more general with regard to the transverse suction distributions handled than has been the case so far. For small and large values of a suction parameter separate exact solutions are obtained which are joined by an approximate solution for arbitrary values of the suction parameter. The approximate solution promises to be useful for intermediate to large values of the parameter.

While it would have been possible in the analysis to take as our reference geometry the radiused corner of arbitrary angle, thereby maximizing the generality of the treatment as far as we are able, we have chosen instead to deal with the rectangular sharp corner. This keeps the development clear of geometrical complications which are more conveniently added at a later stage.

Analysis

Equations of Motion

The corner is shown in Fig. 1. The joining line of the two quarter-infinite plates coincides with the positive x axis of a right-handed Cartesian (x,y,z) coordinate system in which the y and z axes coincide with the leading edges of the plates. The corner is immersed in an infinite incompressible stream whose velocity components are $(U,0,0)$ everywhere except where disturbed by the corner itself, in which case the components are denoted by (u,v,w). The walls are permeable and it is assumed that wall suction is applied which satisfies the following conditions:

$$y=0, \quad z>0^+; \quad v=v_s(x)=0(Re^{-1/2}), \quad (u=w=0)$$

$$y>0^+, \quad z=0; \quad w=v_s(x), \quad (u=v=0) \qquad (1)$$

where 0^+ means arbitrarily small but nonzero. Re is the Reynolds number defined by $Re=UL/\nu$ where L is a length scale $0(x)$ and ν is the kinematic viscosity. Consideration is restricted to situations for which $Re\to\infty$. In this limit the Navier-Stokes and continuity equations for steady in-

Received March 18, 1981; revision received May 24, 1982.

*Lecturer, Dept. of Mechanical Engineering.
†Lecturer, Dept. of Mechanical Engineering.

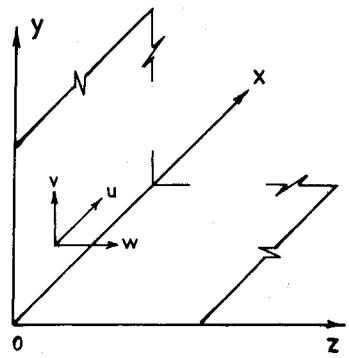

Fig. 1 Cartesian coordinate system.

compressible flow may be written as

$$\sigma u^* \frac{\partial u^*}{\partial \sigma} - (\eta u^* - v^*)\frac{\partial u^*}{\partial \eta} - (\zeta u^* - w^*)\frac{\partial u^*}{\partial \zeta} = \nabla^2 u^* \tag{2a}$$

$$u^*\left(-v^* + \sigma\frac{\partial v^*}{\partial \sigma} - \eta\frac{\partial v^*}{\partial \eta} - \zeta\frac{\partial v^*}{\partial \zeta}\right) + v^*\frac{\partial v^*}{\partial \eta} + w^*\frac{\partial v^*}{\partial \zeta} = \nabla^2 v^* - \frac{\partial p^*}{\partial \eta} \tag{2b}$$

$$u^*\left(-w^* + \sigma\frac{\partial w^*}{\partial \sigma} - \eta\frac{\partial w^*}{\partial \eta} - \zeta\frac{\partial w^*}{\partial \zeta}\right) + v^*\frac{\partial w^*}{\partial \eta} + w^*\frac{\partial w^*}{\partial \zeta} = \nabla^2 w^* - \frac{\partial p^*}{\partial \zeta} \tag{2c}$$

$$\sigma\frac{\partial u^*}{\partial \sigma} - \eta\frac{\partial u^*}{\partial \eta} - \zeta\frac{\partial u^*}{\partial \zeta} + \frac{\partial v^*}{\partial \eta} + \frac{\partial w^*}{\partial \zeta} = 0 \tag{2d}$$

where

$$\sigma = -(2X)^{1/2} Re^{1/2} v_s(X)/U, \quad \eta = (2X)^{-1/2} Y, \quad \zeta = (2X)^{-1/2} Z$$

$$u^*(\sigma,\eta,\zeta) = u(X,Y,Z)/U$$

$$v^*(\sigma,\eta,\zeta) = (2X)^{1/2} Re^{1/2} v(X,Y,Z)/U$$

$$w^*(\sigma,\eta,\zeta) = (2X)^{1/2} Re^{1/2} w(X,Y,Z)/U$$

$$p^* = 2XRep(X,Y,Z)/(\rho U^2), \quad X = x/L$$

$$Y = Re^{1/2} y/L, \quad Z = Re^{1/2} z/L, \quad \nabla^2 \equiv \frac{\partial^2}{\partial \eta^2} + \frac{\partial^2}{\partial \zeta^2}$$

and ρ is the density. The corresponding boundary conditions are

$$\begin{aligned}
&\eta = 0; \quad u^* = 0, && v^* = \sigma v_c^*(\sigma,\zeta), && w^* = 0\\
&\zeta = 0; \quad u^* = 0, && v^* = 0, && w^* = \sigma v_c^*(\sigma,\eta)\\
&\eta \to \infty; \quad u^* = \bar{u}(\sigma,\zeta), && v^* = \bar{w}(\sigma,\zeta), && w^* = \bar{v}(\sigma,\zeta)\\
&\zeta \to \infty; \quad u^* = \bar{u}(\sigma,\eta), && v^* = \bar{v}(\sigma,\eta), && w^* = \bar{w}(\sigma,\eta)
\end{aligned} \tag{3}$$

where $v_c^*(\sigma,\zeta) \equiv -v(X,0,Z)/v_s(X)$. $\bar{u}(\sigma,\eta)$, $\bar{v}(\sigma,\eta)$, $\bar{w}(\sigma,\eta)$ are the solutions of

$$\sigma\bar{u}\frac{\partial \bar{u}}{\partial \sigma} - (\eta\bar{u} - \bar{v})\frac{\partial \bar{u}}{\partial \eta} = \frac{\partial^2 \bar{u}}{\partial \eta^2} \tag{4}$$

$$\sigma\bar{u}\frac{\partial \bar{w}}{\partial \sigma} - (\eta\bar{u} - \bar{v})\frac{\partial \bar{w}}{\partial \eta} - \bar{u}\bar{w} = \lim_{\eta\to\infty}\left(\sigma\frac{\partial \bar{v}}{\partial \sigma} - \bar{v}\right) + \frac{\partial^2 w}{\partial \eta^2} \tag{5}$$

$$\sigma\frac{\partial \bar{u}}{\partial \sigma} - \eta\frac{\partial \bar{u}}{\partial \eta} + \frac{\partial \bar{v}}{\partial \eta} = 0 \tag{6}$$

subject to

$$\bar{u}(\sigma,0) = 0, \qquad \bar{u}(\sigma,\infty) = 1, \qquad \bar{v}(\sigma,0) = -\sigma \tag{7a}$$

$$\bar{w}(\sigma,0) = 0, \qquad \bar{w}(\sigma,\infty) = \bar{v}(\sigma,\infty) \tag{7b}$$

By symmetry, the solutions to Eqs. (4-7) will also be the solutions for $\bar{u}(\sigma,\zeta)$, $\bar{v}(\sigma,\zeta)$, and $\bar{w}(\sigma,\zeta)$.

The condition $\eta = 0$, $v^* = \sigma v_c^*(\sigma,\zeta)$ [Eq. (3)] requires explanation. Equation (1) states that the wall suction is uniform everywhere in the y-z plane except, possibly, in the immediate vicinity of the point $y = z = 0$. On the other hand, the no-slip condition which is assumed to remain in force when suction is employed requires that $v = 0$ on $z = 0$. Expressed in terms of the working variables (and noting that $z = 0^+$ corresponds to $\zeta \to \infty$ as $Re \to \infty$) these conditions are $v^*(\sigma,0,0) = 0$ and $v^*(\sigma,0,\infty) = -\sigma$. The transition between these two limits is represented by $\sigma v_c^*(\sigma,\zeta)$ where

$$v_c^*(\sigma,0) = 0 \text{ and } v_c^*(\sigma,\infty) = -1 \tag{8}$$

The function $v_c^*(\sigma,\zeta)$ is considered to be indeterminate and a solution of Eqs. (2) must involve an assumption for the form of v_c^* satisfying Eq. (8), as well as the prescription of $v_s(X)$. An exactly similar situation exists on the wall $\zeta = 0$, and completing the symmetry implied by Eq. (1) we choose the distribution $w^*(\sigma,\eta,0)$ to be $v_c^*(\sigma,\eta)$. The effect of different choices for v_c^* will be shown later, but henceforth we will assume that $v_s(X) = \text{constant} \le 0$ and that $v_c^*(\sigma,\zeta) = v_c^*(\zeta)$ and $v_c^*(\sigma,\eta) = v_c^*(\eta)$.

Equations (4) and (6) are the equations for the flow over a semi-infinite flat plate and were solved subject to conditions (7a) by Iglisch[10] for uniform suction ($v_s = \text{const}$). Equation (5) with Eqs. (7b) were solved by El-Gamal and Barclay[9] by a step-by-step method in σ starting at $\sigma = 0$ with the known zero suction solution, namely

$$\bar{u}(0,u) = f'(\eta), \quad \bar{v}(0,u) = uf' - f, \quad \bar{w}(0,\eta) = \beta H'(\eta) \tag{9}$$

where $f(\eta)$ is the Blasius function for flow over a semi-infinite flat plate, $H(\eta)$ is a function determined by Rubin,[3] a prime denotes differentiation with respect to η, and $\beta = \lim_{\eta\to\infty}(\eta f' - f) = 1.2168$.

The numerical solution of Eqs. (2) is evidently difficult since they are nonlinear and involve three independent variables. However, when σ is small the nonlinearity in the problem is avoided by treating the flow as a perturbation about the known zero-suction ($\sigma = 0$) solution. Furthermore, it may be assumed with some confidence that the algebraic decay of the corner layer into the boundary layer at $\zeta \to \infty$ or $\eta \to \infty$ and into the potential flow regime, a behavior which is a particular feature of this type of flow, will be entirely accounted for in the base (i.e., zero-suction) solution. Conversely, when σ is sufficiently large, we must expect the flow in the corner layer to assume an asymptotic state corresponding to that existing in the boundary layers at η or $\zeta \to \infty$. In this state the dependence on σ will disappear and a relatively simple problem will result. In the special case of this problem considered by El-Gamal and Barclay[7] algebraic decay was shown to be absent and we will assume that this is generally true when σ is large.

For moderate values of σ where solutions for small or large σ are invalid, an approximate solution for any value of σ will be put forward based on an adaptation of Carrier's[11] treatment of the zero-suction case. The essence of the method

is to replace the streamwise vorticity equation with an assumed relation connecting the crossflow and streamwise velocity components. The accuracy of the method for small and large σ is tested against the exact solutions.

Solution for Small σ

The perturbation method of solution to be adopted here for the corner layer equation (2) involves series expansions of the velocity components and the pressure in terms of powers of σ. This requires a corresponding treatment of the boundary-layer equations (4-7), despite the availability of the step-by-step solution of these equations by El-Gamal and Barclay.[9] Therefore, the solution for small σ is started by reformulating the problem posed by Eqs. (4-7) in the following manner.

Assume that

$$\bar{u}(\sigma,\eta)=\sum_{n=0}^{\infty}\bar{u}_n(\eta)\sigma^n$$

$$\bar{v}(\sigma,\eta)=\sum_{n=0}^{\infty}\bar{v}_n(\eta)\sigma^n$$

$$\bar{w}(\sigma,\eta)=\sum_{n=0}^{\infty}\bar{w}_n(\eta)\sigma^n \tag{10}$$

Substitution of series (10) into Eqs. (4-7) and retaining only terms of order $n=0$ gives the zero-suction situation for which the solution is given by Eq. (9). The solution for $\bar{u}_1$ and $\bar{v}_1$ is also known,[12] and we can show that $\bar{w}_1=\frac{1}{2}\beta H_1'(\eta)$ where

$$H_1'(\eta)=-\frac{2}{\beta}f'f_1(\infty)+f'\int_0^{\infty}\frac{(2\ddot{H}f_1+\dot{H}\dot{f}_1)(1-\dot{f})}{\ddot{f}}\,\mathrm{d}t$$
$$+\int_0^{\eta}\frac{\dot{f}(2\ddot{H}f_1+\dot{H}\dot{f}_1)}{\ddot{f}}\,\mathrm{d}t-f'\int_0^{\eta}\frac{(2\ddot{H}f_1+\dot{H}\dot{f}_1)}{\ddot{f}}\,\mathrm{d}t \tag{11}$$

The function $H_1'(\eta)$ is shown in Fig. 2.

To solve the corner layer equations (2) we assume that

$$u^*=\sum_{n=0}^{\infty}u_0^*(\eta,\zeta)\sigma^n,\qquad v^*=\sum_{n=0}^{\infty}v_n^*(\eta,\zeta)\sigma^n$$

$$\bar{w}^*=\sum_{n=0}^{\infty}w_n^*(\eta,\zeta)\sigma^n,\qquad p^*=\sum_{n=0}^{\infty}p_n^*(\eta,\zeta)\sigma^n \tag{12}$$

Placing Eqs. (12) into Eqs. (2) and retaining only terms of order $n=1$ we have

$$\left(u_0^*-\eta\frac{\partial u_0^*}{\partial\eta}-\zeta\frac{\partial u_0^*}{\partial\zeta}\right)u_1^*+\frac{\partial u_0^*}{\partial\eta}v_1^*+\frac{\partial u_0^*}{\partial\zeta}w_1^*$$
$$-(\eta u_0^*-v_0^*)\frac{\partial u_1^*}{\partial\eta}-(\zeta u_0^*-w_0^*)\frac{\partial u_1^*}{\partial\zeta}=\nabla^2u_1^* \tag{13a}$$

$$-\left(v_0^*+\eta\frac{\partial v_0^*}{\partial\eta}+\zeta\frac{\partial v_0^*}{\partial\zeta}\right)u_1^*+\frac{\partial v_0^*}{\partial\eta}v_1^*+\frac{\partial v_0^*}{\partial\zeta}w_1^*$$
$$-(\eta u_0^*-v_0^*)\frac{\partial v_1^*}{\partial\eta}-(\zeta u_0^*-w_0^*)\frac{\partial v_1^*}{\partial\zeta}=\nabla^2v_1^*-\frac{\partial p_1^*}{\partial\eta} \tag{13b}$$

$$-\left(w_0^*+\eta\frac{\partial w_0^*}{\partial\eta}+\zeta\frac{\partial w_0^*}{\partial\zeta}\right)u_1^*+\frac{\partial w_0^*}{\partial\eta}v_1^*+\frac{\partial w_0^*}{\partial\zeta}w_1^*$$
$$-(\eta u_0^*-v_0^*)\frac{\partial w_1^*}{\partial\eta}-(\zeta u_0^*-w_0^*)\frac{\partial w_1^*}{\partial\zeta}=\nabla^2w_1^*-\frac{\partial p_1^*}{\partial\zeta} \tag{13c}$$

$$u_1^*-\eta\frac{\partial u_1^*}{\partial\eta}-\zeta\frac{\partial u_1^*}{\partial\zeta}+\frac{\partial v_1^*}{\partial\eta}+\frac{\partial w_1^*}{\partial\zeta}=0 \tag{13d}$$

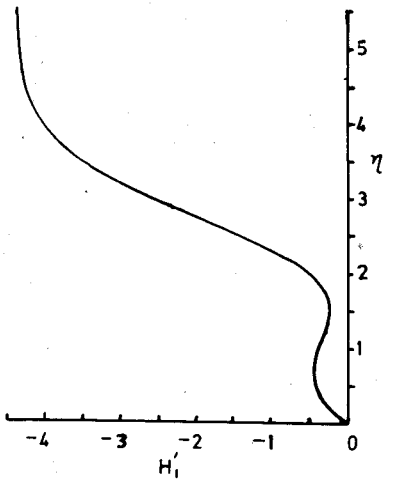

Fig. 2 Small σ solution: $\bar{w}_1=\frac{1}{2}\beta H_1'(\eta)$.

where u_0^*, v_0^*, and w_0^* are the known velocity components for the corner layer flow with no suction ($\sigma=0$).[13]

The boundary conditions for Eqs. (13) are obtained by placing Eqs. (12) into Eqs. (3). They are

$$\eta=0,\ u_1^*=0,\ v_1^*=v_c^*(\zeta),\ w_1^*=0$$

$$\zeta=0,\ u_1^*=0,\ v_1^*=0,\ w_1^*=v_c^*(\eta)$$

$$\eta\to\infty,\ u_1^*=\tfrac{1}{2}f_1'(\zeta),\ v_1^*=\tfrac{1}{2}\beta H_1'(\zeta),\ w_1^*=\tfrac{1}{2}\zeta f_1'(\zeta)-f_1(\zeta)$$

$$\zeta\to\infty,\ u_1^*=\tfrac{1}{2}f_1'(\eta),\ v_1^*=\tfrac{1}{2}f_1'(\eta)-f_1(\eta),\ w_1^*=\tfrac{1}{2}\beta H_1'(\eta) \tag{14}$$

Equations (13) and (14) were solved numerically by choosing

$$v_c^*(t)=e^{-\alpha t}-1,\qquad \alpha=\text{const} \tag{15}$$

Solution for Large σ

As in the case for small σ, the solution is started by assuming that the flow in the boundary layers can be represented by series which for large σ take the form

$$\bar{u}(\sigma,\eta)=\bar{U}(\sigma,\lambda)=\sum_{n=0}^{\infty}U_n(\lambda)\sigma^{-n}$$

$$\bar{v}(\sigma,\eta)=\bar{V}(\sigma,\lambda)=\sum_{n=0}^{\infty}V_n(\lambda)\sigma^{-n+1}$$

$$\bar{w}(\sigma,\eta)=\bar{W}(\sigma,\lambda)=\sum_{n=0}^{\infty}W_n(\lambda)\sigma^{-n+1} \tag{16}$$

where λ is a new coordinate to replace η and is defined as

$$\lambda=\sigma\eta=-v_s y/\nu$$

Substitution of Eqs. (16) in Eqs. (4-7) and solving for the leading terms gives

$$U_0=1-e^{-\lambda},\qquad V_0=-1,\qquad W_0=e^{-\lambda}-1 \tag{17}$$

in which U_0 and V_0 were previously obtained by Griffith and Meredith.[8]

Within the corner layer we assume that

$$u^*(\sigma,\eta,\zeta)=\sum_{n=0}^{\infty}U_n(\lambda,\Omega)\sigma^{-n}$$

$$v^*(\sigma,\eta,\zeta) = \sum_{n=0}^{\infty} V_n(\lambda,\Omega)\,\sigma^{-n+1}$$

$$w^*(\sigma,\eta,\zeta) = \sum_{n=0}^{\infty} W_n(\lambda,\Omega)\,\sigma^{-n+1}$$

$$p^*(\sigma,\eta,\zeta) = \sum_{n=0}^{\infty} P_n(\lambda,\Omega)\,\sigma^{-n+2} \tag{18}$$

where n is even and $\Omega=\sigma\zeta$.

When Eqs. (18) are placed in Eqs. (2) and (3) and only the leading terms are retained the corner layer equations become

$$V_0\frac{\partial U_0}{\partial\lambda} + W_0\frac{\partial U_0}{\partial\Omega} = \bar{\nabla}^2 U_0 \tag{19a}$$

$$V_0\frac{\partial V_0}{\partial\lambda} + W_0\frac{\partial V_0}{\partial\Omega} = \bar{\nabla}^2 V_0 - \frac{\partial P_0}{\partial\lambda} \tag{19b}$$

$$V_0\frac{\partial W_0}{\partial\lambda} + W_0\frac{\partial W_0}{\partial\Omega} = \bar{\nabla}^2 W_0 - \frac{\partial P_0}{\partial\Omega} \tag{19c}$$

$$\frac{\partial V_0}{\partial\lambda} + \frac{\partial W_0}{\partial\Omega} = 0 \tag{19d}$$

where

$$\bar{\nabla}^2 \equiv \frac{\partial^2}{\partial\lambda^2} + \frac{\partial^2}{\partial\Omega^2}$$

and the boundary conditions are

$$\lambda=0;\ U_0=0,\ V_0=V_0^*(\Omega)=v_c^*(\zeta),\ W_0=0$$

$$\Omega=0;\ U_0=0,\ V_0=0,\ W_0=W_0^*(\lambda)=v_c^*(\eta)$$

$$\lambda\to\infty;\ U_0=1-e^{-\Omega},\ V_0=e^{-\Omega}-1,\ W_0=-1$$

$$\Omega\to\infty;\ U_0=1-e^{-\lambda},\ V_0=-1,\ W_0=e^{-\lambda}-1 \tag{20}$$

The last three of Eqs. (19) are uncoupled from the first and the crossflow velocities may therefore be determined without regard to the streamwise velocity component U_0. The equations for the crossflow are reduced to a single equation by differentiating the second and third Eqs. (19) with respect to Ω and λ, respectively, subtracting the results to eliminate P_0, and introducing the streamfunction ψ to satisfy Eq. (19d) identically where ψ is such that

$$V_0 = \frac{\partial\psi}{\partial\Omega}, \qquad W_0 = -\frac{\partial\psi}{\partial\lambda} \tag{21}$$

The last three of Eqs. (19) then become

$$\frac{\partial^4\psi}{\partial\lambda^4} + \frac{\partial^4\psi}{\partial\Omega^4} + 2\frac{\partial^4\psi}{\partial\lambda^2\partial\psi^2} + \frac{\partial\psi}{\partial\lambda}\left(\frac{\partial^3\psi}{\partial\Omega\partial\lambda^2} + \frac{\partial^3\psi}{\partial\Omega^3}\right) - \frac{\partial\psi}{\partial\Omega}\left(\frac{\partial^3\psi}{\partial\lambda\partial\Omega^2} + \frac{\partial^3\psi}{\partial\lambda^3}\right) = 0 \tag{22}$$

and from Eqs. (20) the boundary conditions are

$$\lambda=0;\qquad \frac{\partial\psi}{\partial\Omega} = V_0^*(\Omega), \qquad \frac{\partial\psi}{\partial\lambda} = 0$$

$$\Omega=0;\qquad \frac{\partial\psi}{\partial\Omega} = 0, \qquad \frac{\partial\psi}{\partial\lambda} = -W_0^*(\lambda)$$

$$\lambda\to\infty;\qquad \frac{\partial\psi}{\partial\Omega} = e^{-\Omega}-1, \qquad \frac{\partial\psi}{\partial\lambda} = 1$$

$$\Omega\to\infty;\qquad \frac{\partial\psi}{\partial\Omega} = -1, \qquad \frac{\partial\psi}{\partial\lambda} = 1-e^{-\lambda} \tag{23}$$

Before remarking on the general method of solving Eqs. (22) and (23), we draw attention to the particularly simple solution obtained by El-Gamal and Barclay[7] which results from the following special choice for $V_0^*(\Omega)$ and $W_0^*(\lambda)$:

$$V_0^*(\Omega) = e^{-\Omega}-1, \qquad W_0^*(\lambda) = e^{-\lambda}-1 \tag{24}$$

This yields the solution

$$\psi = \lambda - \Omega + e^{-\lambda} - e^{-\Omega} \tag{25}$$

as may be verified by direct substitution in Eqs. (22) and (23).

It follows from Eqs. (21) and (25) that $V_0(\lambda,\Omega) = V_0^*(\Omega)$ and $W_0(\lambda,\Omega) = W_0^*(\lambda)$ for all λ and Ω when $V_0^*(\Omega)$ and $W_0^*(\lambda)$ are given by Eqs. (24). Substituting these results into Eq. (19a) gives

$$\bar{\nabla}^2 U_0 + (1-e^{-\Omega})\frac{\partial U_0}{\partial\lambda} + (1-e^{-\lambda})\frac{\partial U_0}{\partial\Omega} = 0 \tag{26}$$

which was solved numerically subject to the conditions (20).

The solution of the biharmonic Eq. (22) for ψ for arbitrarily chosen distributions of V_0 and $\lambda=0$ (and, symmetrically, W_0 on $\Omega=0$) generally has to be carried out numerically, but a direct approach is rather difficult. Instead, it was found more convenient to return to the velocity components V_0, W_0, and to introduce the streamwise vorticity component ω, where

$$\omega = -\bar{\nabla}^2\psi = \frac{\partial W_0}{\partial\lambda} - \frac{\partial V_0}{\partial\Omega} \tag{27}$$

so that Eq. (22) becomes

$$\bar{\nabla}^2\omega - V_0\frac{\partial\omega}{\partial\lambda} - W_0\frac{\partial\omega}{\partial\Omega} = 0 \tag{28}$$

Differentiating Eq. (27) with respect to λ and using Eq. (19d) gives

$$\bar{\nabla}^2 W_0 = \partial\omega/\partial\lambda \tag{29}$$

In a similar way

$$\bar{\nabla}^2 V_0 = -\partial\omega/\partial\Omega \tag{30}$$

Equations (27-30), satisfying Eq. (20), were solved numerically with v_c^* given by Eq. (15). The crossflow solution was then used in Eq. (19a) to find U_0.

Approximate Solutions for Arbitrary σ

For values of σ outside the range of validity of the small and large σ solutions, and in the absence of a more rigorous method, we consider an adaptation of a scheme used by Carrier[11] in his treatment of the zero suction problem. With $\sigma=0$, Carrier neglected the second and third of Eqs. (2) and compensated (imperfectly) for the indeterminacy thus introduced by assuming a single stream function $g_c(\eta,\zeta)$ to have the following properties

$$u^* = \partial^2 g_c/\partial\eta\partial\zeta, \quad v^* = \eta u^* - \partial g_c/\partial\zeta, \quad w^* = \zeta u^* - \partial g_c/\partial\eta$$

Substitution for u^*, v^*, w^* in terms of g_c satisfies Eq. (2d) identically, leaving Eq. (2a) to be solved for g_c. Un-

fortunately, not all of the boundary conditions can be satisfied by this method and since v^* and w^* do not automatically take the correct form at $\eta\to\infty$ and $\zeta\to\infty$, respectively, then they are incorrect there. We know, for example, that the correct form for w^* as $\zeta\to\infty$ is $\beta H'(\eta)$ [Eq. (9)], and since this is markedly different from the form actually used‡ it is to be expected that the solution will not be entirely satisfactory.

In using Carrier's method we shall, in general, incur the same defects but not necessarily with the same consequences. In any case we can test the method against the known exact solutions for small and large σ, and the unconstrained boundary values against the known exact conditions for all σ and thereby gage the likely accuracy of the method for σ values beyond the ranges of the exact solutions.

For the corner layer we assume that

$$u^*(\sigma,\eta,\zeta)=g_{\eta\zeta}(\sigma,\eta,\zeta)$$

$$v^*=-\frac{\sigma}{2}g_{\sigma\zeta}+\eta g_{\eta\zeta}-g_\zeta$$

$$w^*=-\frac{\sigma}{2}g_{\sigma\eta}+\zeta g_{\eta\zeta}-g\eta \tag{31}$$

where a suffix σ, η, or ζ denotes differentiation with respect to that variable.

Equation (2d) is satisfied identically [but not in its asymptotic form, Eq. (6)]. Disregarding Eqs. (2b) and (2c) and substituting from Eq. (31) in Eq. (2a) we have

$$\sigma g_{\eta\zeta}g_{\sigma\eta\zeta}-\left(\frac{\sigma}{2}g_{\sigma\zeta}+g_\zeta\right)g_{\eta\eta\zeta}-\left(\frac{\sigma}{2}g_{\sigma\eta}+g_\eta\right)g_{\eta\zeta\zeta}=g_{\eta\eta\eta\zeta}+g_{\eta\zeta\zeta\zeta} \tag{32}$$

When $\sigma=0$ Eq. (32) is the same as that solved by Carrier. When $\sigma\to\infty$ Eq. (32) takes the following form (in the notation for large σ)

$$\bar\nabla^2 U_0-V_0(\Omega)\frac{\partial U_0}{\partial\lambda}-W_0(\lambda)\frac{\partial U_0}{\partial\Omega}=0 \tag{33}$$

This is different from the exact limit, Eq. (19a), but it has been shown to be correct for the special choice of suction distribution prescribed by Eq. (24). Otherwise the dependence on σ complicates the matter. A step-by-step solution in the σ direction might be used were it not for the somewhat excessive amount of computing required. Instead, a method found to be successful in two-dimensional flows[14] is adapted to suit the three-dimensionality of the present problem.

Denoting $\partial g/\partial\sigma$ by h and differentiating Eq. (32) with respect to σ gives

$$h_{\eta\eta\eta\zeta}+h_{\eta\zeta\zeta\zeta}+g_\zeta h_{\eta\eta\zeta}+g_\eta h_{\eta\zeta\zeta}-g_{\eta\zeta}h_{\eta\zeta}+\frac{3}{2}h_\zeta g_{\eta\eta\zeta}+\frac{3}{2}h_\eta g_{\eta\zeta\zeta}=\sigma\frac{\partial}{\partial\sigma}\left[g_{\eta\zeta}h_{\eta\zeta}-\frac{1}{2}h_\zeta g_{\eta\eta\zeta}-\frac{1}{2}h_\eta g_{\eta\zeta\zeta}\right] \tag{34}$$

In correspondence with the two-dimensional case we make the simplifying assumption that the right-hand side of Eq. (34) is negligibly small in relation to terms on the left-hand side, i.e., we assume that

$$h_{\eta\eta\eta\zeta}+h_{\eta\zeta\zeta\zeta}+g_\zeta h_{\eta\eta\zeta}+g_\eta h_{\eta\zeta\zeta}-g_{\eta\zeta}h_{\eta\zeta}+\frac{3}{2}h_\zeta g_{\eta\eta\zeta}+\frac{3}{2}h_\eta g_{\eta\zeta\zeta}=0 \tag{35}$$

‡When $\zeta\to\infty$, w^* in Carrier's analysis varies as $[f'(\eta)+F'(\eta)]$ where F' is a positive term, small but not negligible compared with f'.

Equations (32) and (35) are the determining equations for the dependent variables g and h, and adopting Eq. (15) they were solved subject to the following boundary conditions

$$\begin{aligned}
&\eta=0;\quad g_{\eta\zeta}=0,\quad g_\zeta=-\frac{2}{3}\sigma v_c^*(\zeta),\quad g_\eta=0\\
&\qquad h_{\eta\zeta}=0,\quad h_\zeta=-\frac{2}{3}v_c^*(\zeta),\quad h_\eta=0\\
&\zeta=0;\quad g_{\eta\zeta}=0,\quad g_\zeta=0,\quad g_\eta=-\frac{2}{3}\sigma v_c^*(\eta)\\
&\qquad h_{\eta\zeta}=0,\quad h_\zeta=0,\quad h_\eta=-\frac{2}{3}v_c^*(\eta)\\
&\eta\to\infty;\quad g_{\eta\zeta}=\bar u(\sigma,\zeta),\quad h_{\eta\zeta}=\frac{\partial\bar u}{\partial\sigma}(\sigma,\zeta)\\
&\zeta\to\infty;\quad g_{\eta\zeta}=\bar u(\sigma,\eta),\quad h_{\eta\zeta}=\frac{\partial\bar u}{\partial\sigma}(\sigma,\eta)
\end{aligned} \tag{36}$$

Results

Solutions were obtained by finite difference methods, usually using a mesh interval of 0.4 in each of the independent variables. A solution was deemed to be realized when every dependent variable at each mesh point changed by less than 0.0001 in successive iterations.

Small σ

The numerical results are exemplified by Figs. 3-5. Figure 3 shows the perturbation velocity component u_1^* in planes parallel to the symmetry plane when $\alpha=10$ which for the numerical solution approximates to constant v_c^* for η or $\zeta>0$. The effect of suction is evident. The maximum amplitude occurs in the plane of symmetry where u_1^* attains a peak value approximately 70% greater than at $\zeta\to\infty$. Near the intersection of the corner, however, the magnitude of u_1^* is smaller than it is elsewhere near the solid surface, whereas we would prefer to see the converse being true in the interest of maximum benefit for the stability of the corner layer. The retention of the no-slip condition for the suction velocity is

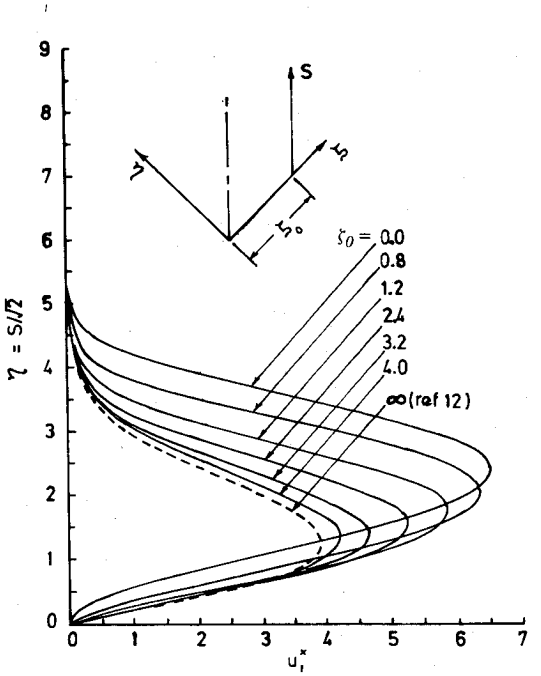

Fig. 3 Small σ solution: perturbation velocity function u_1^* for planes parallel to the symmetry plane.

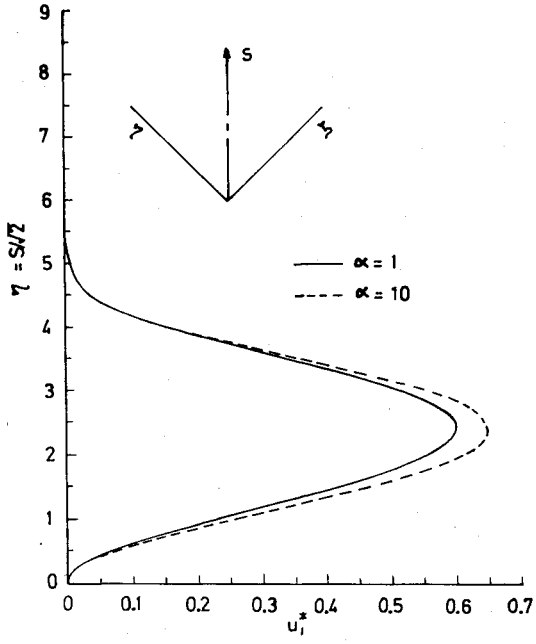

Fig. 4 Effect of α on $u_1^*(\eta,\eta)$.

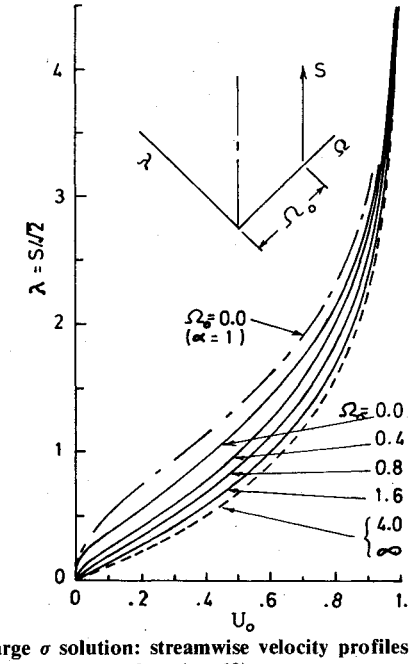

Fig. 6 Large σ solution: streamwise velocity profiles U_0 in planes parallel to the symmetry plane ($\alpha = 10$).

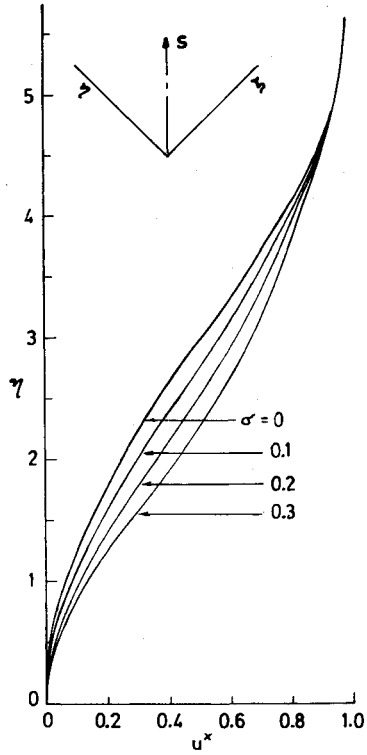

Fig. 5 Small σ solution: streamwise velocity profiles in symmetry plane.

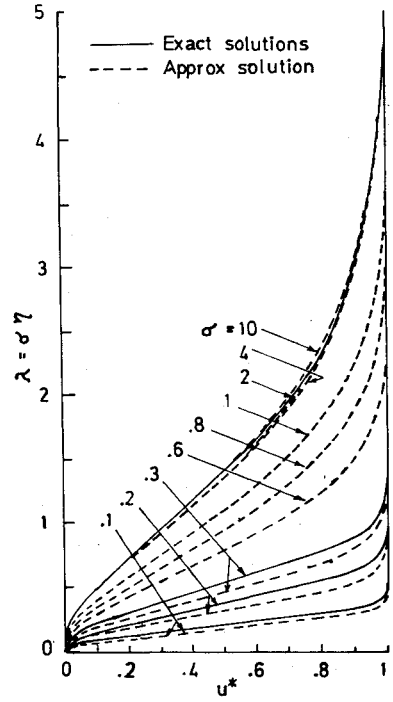

Fig. 7 Comparison of exact solutions for u^* in the plane of symmetry for small and large σ and the approximate solution.

probably important here since it results in the suction velocity vector being zero at the intersection line where its effect is most needed. Nevertheless, there is little doubt from the results that the corner layer will be influenced beneficially by suction.

The effect on the symmetry plane distribution of u_1^* of changing the value of α from 10 to 1 is shown in Fig. 4. The change in $v_c^*(\zeta)$ due to the decrease in α is significant for $0 \leq \zeta \lesssim 2$ but the consequence for u_1^* is small and suggests that more general forms of v_c^* when used will lead to approximately the same results as for the special form used here.

Figure 5 shows $u^* = u_0^* + \sigma u_1^*$ in the symmetry plane for different values of σ and $\alpha = 10$.

Large σ

Figure 6 shows the results for U_0 in different planes parallel to the symmetry plane of the corner for $\alpha = 10$. In the same figure the profile of U_0 in the symmetry plane when $\alpha = 1$ is shown for comparison, the crossflow used in the derivation being calculated numerically rather than taken from Eq. (25). Once again, the large change in the value of α has only a modest effect on U_0.

One reason for calculating the crossflow numerically when $\alpha = 1$ was to compare the results so obtained with the analytical solution, Eq. (25), and thereby determine the accuracy of the numerical method, particularly with regard to the adequacy of the mesh size used. Using mesh sizes of 0.8 and 0.4 the results showed 0.4 to be completely satisfactory.

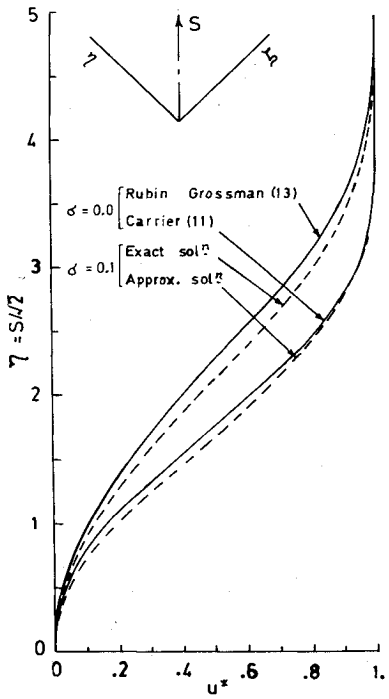

Fig. 8 Comparison of exact and approximate solutions for u^* in the plane of symmetry when $\sigma = 0$ and 0.1.

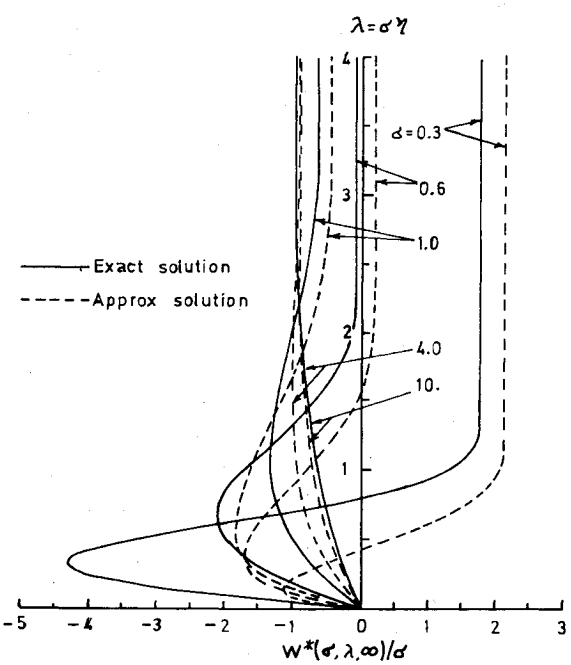

Fig. 9 Comparison of exact[9] and approximate crossflow component $w^*(\sigma, \lambda, \infty)/\sigma$ at the side edge of the corner layer for different values of σ.

Arbitrary σ (Approximate Solution)

The solution to Eqs. (32) and (35) using Eq. (15) with $\alpha = 10$ is illustrated by Fig. 7, which shows the streamwise velocity component u^* for σ ranging from 0.1 to 10. The results of the exact solutions for small and large σ are also shown in the same figure for comparison.

When σ is small (<0.3, say) the relation between the approximate and exact solutions is much the same as that when $\sigma = 0$. This is clearly shown in Fig. 8 where the results for $\sigma = 0$ and 0.1 are drawn with respect to the coordinate η. (The coordinate λ used in Fig. 7 is the most convenient when $\sigma > 0$ but is inappropriate when $\sigma = 0$.)

When $\sigma \to \infty$ it has been shown that the approximate solution should coincide with the exact solution when $V_0^*(\Omega) = e^{-\Omega} - 1$ and $W_0^*(\lambda) = e^{-\lambda} - 1$. That the approximate and exact solutions are also practically the same for sufficiently large σ when $\alpha = 10$ (and therefore, presumably, for all $\alpha > 1$) is adequately demonstrated by Fig. 7.

Insofar as Carrier's solution for $\sigma = 0$ is considered to be unsatisfactory, the results of the approximate solution presented here for small σ must be considered likewise and therefore we would use the exact result in that region. For large σ, however, the approximate solution is in excellent quantitative agreement with the exact asymptotic solution. The approximate solution for arbitrary σ therefore varies from poor to excellent as σ ranges from small to large values. Furthermore it is shown in Fig. 9 that for the crossflow at the side edge of the corner layer the agreement between the exact[9] and approximate solutions here improves uniformly as σ increases. Consequently there is the strong inference to be drawn that the approximate solution for arbitrary σ throughout the corner also improves uniformly toward its excellent condition at large σ. For this reason it is believed that for values of σ beyond the range of validity of the exact solution for small σ, the Carrier-type approximate solution will provide practically useful data, and increasingly so as σ increases.

References

[1] Zamir, M. and Young, A. D., "Experimental Investigation of the Boundary Layer in a Streamwise Corner," *Aeronautical Quarterly,* Vol. 21, Pt. 4, 1970, pp. 313-339.

[2] Barclay, W. H., "Experimental Investigation of the Laminar Flow along a Straight 135° Corner," *Aeronautical Quarterly,* Vol. 24, Pt. 2, 1973, pp. 147-154.

[3] Rubin, S. G., "Incompressible Flow along a Corner," *Journal of Fluid Mechanics,* Vol. 26, Pt. 1, 1966, pp. 97-110.

[4] Pal, A. and Rubin, S. G., "Asymptotic Features of Viscous Flow along a Corner," *Quarterly of Applied Mathematics,* Vol. 29, No. 91, 1971, pp. 91-108.

[5] Barclay, W. H. and Ridha, A. H., "Flow in Streamwise Corners of Arbitrary Angle," *AIAA Journal,* Vol. 18, Dec. 1980, pp. 1413-1420.

[6] Barclay, W. H., "Flow in Streamwise Corners Having Large Transverse Curvature," *AIAA Journal,* Vol. 20, May 1982, pp. 726-728.

[7] El-Gamal, H. A. and Barclay, W. H., "Laminar Streamwise Corner Flow with Suction," *The Aeronautical Journal,* Vol. 79, Oct. 1975, pp. 466-469.

[8] Griffith, A. A. and Meredith, F. W., "The Possible Improvement in Aircraft Performance Due to the Use of Boundary Layer Suction," RAE Report No. E3501, March 1936, pp. 1-12.

[9] El-Gamal, H. A. and Barclay, W. H., "Crossflow Development at the Side Edges of a Corner Boundary Layer Subjected to Suction," *The Aeronautical Journal,* Vol. 79, Dec. 1975, pp. 550-554.

[10] Iglisch, R., "Exact Calculation of Laminar Boundary Layer in Longitudinal Flow over a Flat Plate with Homogeneous Suction," NACA TM 1205, 1949, pp. 1-69.

[11] Carrier, G. F., "The Boundary-Layer in a Corner," *Quarterly of Applied Mathematics,* Vol. 4, No. 4, 1947, pp. 367-370.

[12] Libby, P. A. and Fox, H., "Some Perturbation Solutions in Laminar Boundary Layer Theory. Part I, The Momentum Equation," *Journal of Fluid Mechanics,* Vol. 17, Nov. 1963, pp. 433-449.

[13] Rubin, S. G. and Grossman, B., "Viscous Flow along a Corner: Part II. Numerical Solution of the Corner Layer Equations," *Quarterly of Applied Mathematics,* Vol. 29, No. 2, 1971, pp. 169-186.

[14] Sparrow, E. M., Quack, H., and Boerner, C. J., "Local Non-Similarity Boundary Layer Solutions," *AIAA Journal,* Vol. 8, Nov. 1970, pp. 1936-1941.